JOURNAL OF IRON AND STEEL RESEARCH, INTERNATIONAL. 2007, 14(1): 42-46

Analysis of Laser Surface Hardened Layers of Automobile Engine Cylinder Liner

LIU Xiu-bo[1,2], YU Gang[1], GUO Jian[2], SHANG Quan-yi[2], ZHANG Zhen-guo[2], GU Yi-jie[3]
(1. Laboratory for Laser Intelligent Manufacturing, Institute of Mechanics, Chinese Academy of Sciences, Beijing 100080, China; 2. School of Materials and Chemical Engineering, Zhongyuan Institute of Technology, Zhengzhou 450007, Henan, China; 3. College of Materials Science and Engineering, Shandong University of Science and Technology, Qingdao 266510, Shandong, China)

Abstract: Gray cast iron that is used for automobile engine cylinder liners was laser surface hardened using Nd : YAG quasi-continuous and CO_2 continuous wave laser, respectively. The macromorphology and microstructure of the laser surface hardened layers were investigated using an optical microscope. Geometric dimensions including depth and width and microhardness distribution of the hardened layers were also examined in order to evaluate the quality of the hardened layers.

Key words: gray cast iron; laser surface hardening; microstructure; hardness

The newly developed laser processing technology has generated considerable interests both in research and industrial application fields, especially as advanced and green manufacturing tools for hard facing or surface repairing in modern automobile industry[1]. However, to date, the main focus in laser surface hardening is on CO_2 laser, which exhibits a low coupling interaction with metal materials due to the relatively longer laser output wavelength. Thus, painting is necessary to increase the absorbing rate before laser radiation. This not only needs additional procedure in the product line but also brings about pollution and hazardous effects to the environment. On the contrary, Nd : YAG laser is emerging as a competitive tool in surface modification due to the short wavelength and high absorbing rate of the metal materials[2].

The aim of this study is to examine the surface hardened layers, which were processed using Nd : YAG quasi-continuous and CO_2 continuous wave laser, respectively. The macromorphology and microstructure of the laser surface hardened layers were investigated using optical microscope. The results and the quality of the hardening layers processed by the two kinds of lasers were compared. Certain methods are proposed and their prospects are also reviewed.

1 Experimental

The material used in this study was pearlite gray cast iron. It is suitable for laser surface hardening and is mainly used in engine cylinders and other tribological moving components in the automobile industry. The laser processing experiments were carried out using a Nd : YAG quasi-continuous and a CO_2 continuous wave laser, respectively. The laser beam had a circular cross-section and the power distribution within them followed the TEM_{01} mode. The laser processing conditions and surface preparation used in the experiments are shown in Table 1. Specimens for metallographic examination by optical microscopy (mode: Nephot-Ⅱ) were cut perpendicular to the beam direction. All the specimens were ground and polished. Etching was performed using 4% Nital reagents. Microhardness was measured by a Ⅱ MF-3 type microhardmeter, which is expressed as a function of depth and width for all the laser processed specimens using a load of 0.1 kg.

Biography: LIU Xiu-bo(1968-), Male, Associate Professor; **E-mail**: liubobo0828@yahoo.com.cn; **Revised Date**: July 20, 2005

Table 1 Processing conditions and surface preparation used in experiments for gray cast iron

Specimen number	Beam power/W	Travel speed/(mm · min^{-1})	Beam diameter/mm	Surface precoating
22	1 600	1 800	3.0	None
24	1 500	1 800	3.0	None
26	1 600	2 200	3.0	None
27	1 800	2 400	3.0	None
30	1 500	3 120	3.0	Graphite coated

Note: Specimen 30 was processed using a CO_2 continuous laser, while all the other three specimens were processed using an Nd : YAG quasi-continuous laser.

2 Results and Discussion

2.1 Geometric features of laser surface hardened layers

Fig. 1 shows the typical geometric dimensions of the laser surface hardened layers. Specimen 26 and 24 were processed using a Nd : YAG quasi-continuous laser, resulting in the depth of 0.15 mm, 0.20 mm and width of 2.3 mm, 2.35 mm of the hardened layers, respectively. However, Specimen 30 processed using a continuous CO_2 laser has a layer with depth of 0.26 mm and width of 3.6 mm. The reason for the above-mentioned measured results can be explained as follows: Since the Nd : YAG is a quasi-continuous laser, the beam size and the pulsed frequency are lower than those for the CO_2 continuous laser, and if the specimens were processed with similar parameters, the energy absorbed by the specimen was low, leading to lower hardened layer depth and width compared to that processed with CO_2 continuous laser. As for Specimens 26 and 24, the difference between them is the processing parameters. The scanning speed for Specimen 26 was 2 200 mm/min, which was more than that for Specimen 24 (1 800 mm/min). The faster the scanning speed, the lesser the interaction time between the laser beam and the materials, thus the less the heat input to the specimen and the less the transformation zone of the specimen. Therefore, the specimen would have a shallower hardened layer.

2.2 Microstructure of laser surface hardened layers

In general, the microstructure of the laser surface hardened layers is a result of the following process. First, the specimen is quickly heated and most of the starting pearlite is transferred into austenite. The austenite then changes into martensite during subsequent rapid cooling, including certain unchanged austenite that is retained. Moreover, if there exists certain phosphorous eutectic in the laser impact area, then it is dissolved and transferred into ledeburite or coarse needle-shaped martensite due to their low melting point. Sheet graphite can be partly dissolved and diffused as a result of the boundary reaction due to a very high temperature. Thus, the typical microstructure of the laser surface hardened layer is composed of martensite or ledeburite, retained austenite, and graphite sheets.

As can be seen from Fig. 2 (a) and (b), the microstructure of the typical hardened layer can be roughly divided into two regions, namely, the phase transformation zone and the transition zone. The top surface area of the hardened layer observed by the OM, shows a uniform and bright white color to be the martensite, and austenite is retained due to the rapid cooling of the high temperature austenite. The area adjacent to the white area was identified as the transformed coarse needle-shaped martensite and some dissolved graphite [Fig. 2 (b)]. The dissolved graphite in this area is evidently thin and short compared to the starting coarse sheet graphite material. The

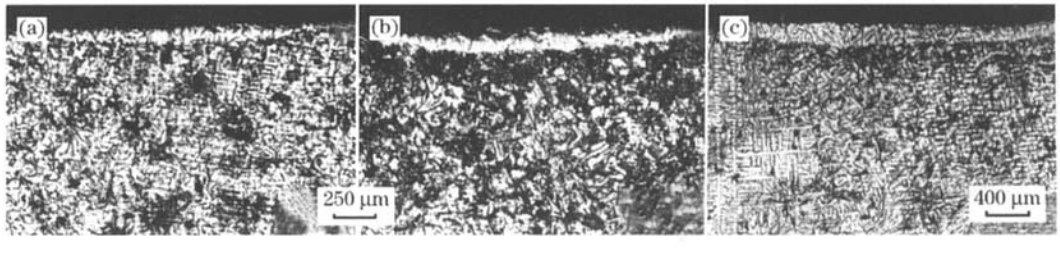

(a) Specimen 26, d=0.15 mm, W=2.3 mm; (b) Specimen 24, d=0.2 mm, W=2.35 mm; (c) Specimen 30, d=0.26 mm, W=3.6 mm

Fig. 1 Cross-sectional images of specimens showing geometric dimensions of hardened layers (d: depth, W: width)

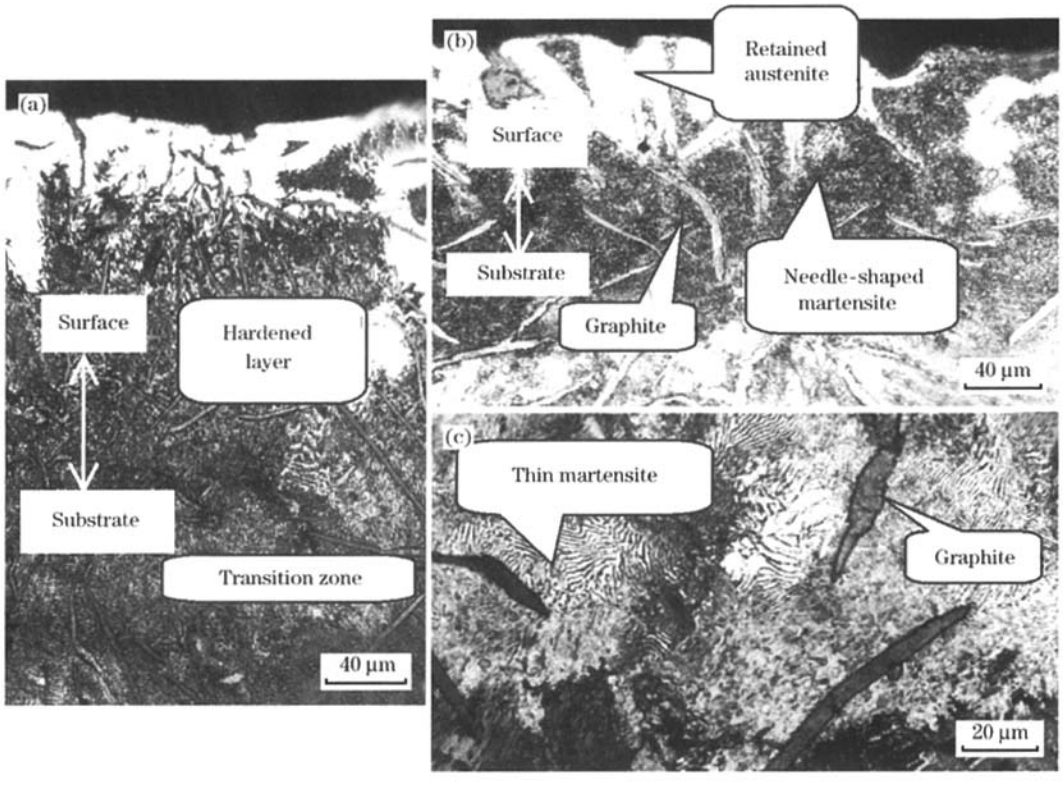

(a) Typical microstructure for Specimen 22; (b) Typical microstructure for Specimen 30; (c) Magnification of microstructure of Specimen 24 in middle of hardened layer of transition zone, showing coarse sheet graphite and pearlite-like thin martensite

Fig. 2 Optical microscope micrographs of gray cast iron after laser surface hardening processing

reason for this phenomenon was due to the rather short interaction time. The graphite′s dissolution in the area was incomplete and may be brought to the upper area and broken into pieces because of the buoyancy and dynamic forces.

An important phenomenon that occurred in the hardened layer was that the morphological characteristic of the microstructure was similar to that of the lamellar pearlite, but the hardness testing showed that its average hardness was 680—700 HV, which indicates that martensite phase transformation had occurred. This was due to the hindering and segregation effects of the sheet carbide (cementite). The high temperature austenite and the subsequent cooling transformation products could only be formulated within the very narrow sheet cementite, leading to the formation of the extremely thin martensite [Fig. 2 (c)][3]. Another important characteristic of phase transformation of the gray cast iron was its eutectic-type microstructure (Fig. 3). Since several graphite sheets existed in gray cast iron, there also existed several graphite-ferrite area. Ferrite transferred into austenite during the rapid heating process. Thus, slight melting phenomenon occurred in the graphite-austenite interphase area. Although the heating temperature was below the melting point of the bulk cast iron, the actual heating temperature might exceed the melting point slightly, leading to a minor melting of the graphite-austenite initially. As the rim of the graphite sheet dissolved, the carbon concentration in the surrounding area increased to a large extent. Thus the eutectic-type mi-

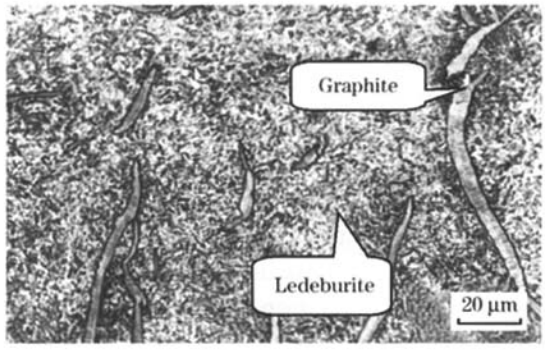

Fig. 3 Eutectic characteristics during phase transformation process of Specimen 27

crostructure was formed in the minor area in the starting graphite-ferrite interphase. As shown in Fig. 3, the ledeburite microstructure which is the eutectics of cementite and pearlite, was formed in the starting graphite-ferrite interphase area[3].

2.3 Microhardness of laser surface hardened layer

Fig. 4 (a) and (b) show the variation of microhardness with depth and width of the laser surface hardened Specimen 26.

The laser surface hardening processing yields a unique, thin microstructure, and most of them is supersaturated solid solution—very hard martensite and there exists a large amount of retained austenite, eliminating the soft graphite at the top surface. The retained austenite is strengthened to a large extent through dislocation and solid-solution strengthening mechanism. So, it is naturally anticipated that the hardened layers contain a very high and uniform hardness distribution.

From the microhardness examination, it is apparent that the microhardness level in the hardened layer, which averages about 700 HV, is significantly higher than that at the substrate region, which averages about 200 HV. It is impotant that the microhardness distribution corresponds to the abovementioned microstructure analysis. It can be seen very clearly from Fig. 4 (a) and (b) that the hardened layer's depth and width are 0.15 mm and 2.3 mm, respectively. Since the top surface (bright white area) of the hardened layer mainly consists of retained austenite, the hardness therein is relatively slightly lower than that of the adjacent area, which shows the highest hardness due to its very hard martensite phase. Moreover, in the transition zone, the microhardness starts to decrease as the microstructure is mainly composed of unchanged pearlite and graphite phases. Fig. 3 (b) shows that the hardness parallel to the surface, which fluctuates to a certain extent due to the fact that at a particular time, the tested area chiefly is a very hard martensite phase and at another point of time, the tested area may be a soft graphite phase to a large extent. However, microhardness distribution of this specimen within the hardened layer is uniform and statistical constant about a mean level.

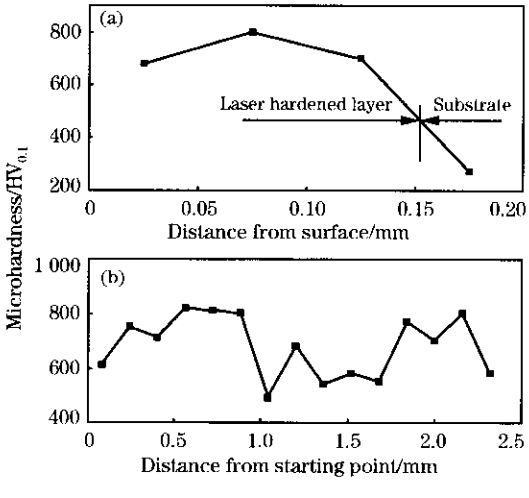

Fig. 4 Variation of microhardness with depth (a) and width (b) of hardened Specimen 26

Since the laser surface hardened layers of the gray cast iron exhibit favorable microstructure characteristic and very high hardness distribution, the quality of the hardened layers is high. It is anticipated that the hardened layers have a very good wear resistance under tribological moving service conditions. It shows that the laser surface hardening is a very promising and economic technique in the automobile industry.

3 Conclusions

(1) The laser surface hardened layers of gray cast iron mainly consist of two zones: hardened zone and transition zone. The depth and width of the hardened layer are related to the laser mode, processing parameters, and so on. CO_2 continuous wave laser yields a relatively deeper and wider hardened layer than that of the Nd : YAG quasi-continuous laser under the same processing conditions. The depth of the hardened layer decreases if the processing scanning speed increases in the same laser mode. But from the long-term point of view, Nd : YAG laser would become the competitive tool in surface hardening due to its high absorbing rate and high production efficiency.

(2) Laser surface hardening for gray cast iron produces a predominant martensite, or/and ledeburite eutectic, including certain retained austenite and certain changed and unchanged graphite microstructures. The corresponding microhardness distribution shows the significantly enhanced hardness of the hardened layers and confirms the results of the microstructure analysis. It is expected that the laser surface hardened layers for gray cast iron should have good wear resistance under tribological service conditions, and therefore laser surface hardening is a promising and economic technique in the automobile

industry.

References:

[1] GUAN Zhen-zhong. Handbook of Laser Processing [M]. Beijing: China Metrology Press, 1998.

[2] Lawrence J, Li L. Modification of the Wettability Characteristics of Polymethyl Methacrylate (PMMA) by Means of CO_2, Nd: YAG, Excimer and High Power Diode Laser Radiation [J]. Materials Science and Engineering, 2001, A303: 142-149.

[3] LIU Jiang-long. High Energy Beam Heat-Treatment [M]. Beijing: China Mechanical Press, 1997.

(Continued from Page 32)

[4] Rade Ognjanovic, Keith Waterson. Finite Element Analysis Modeling of Ingot Refusal Conditions During the Rolling Process [J]. Computers and Structures, 2003, 81(8-11): 871-877.

[5] Grass H, Krempaszky C, Reip T, et al. 3-D Simulation of Hot Forming and Microstructure Evolution [J]. Computational Materials Science, 2003, 28(3-4): 469-477.

[6] Sun C G, Park H D, Hwang S M. Prediction of 3D Strip Temperatures Through the Entire Finishing Mill in Hot Strip Rolling by Finite Element Method [J]. ISIJ International, 2002, 42(6): 629-635.

[7] LAN Yong-jun, CHEN Xiang-yong, HUANG Cheng-jiang, et al. Numerical Simulation and Experimental Verification of Temperature Distribution in Hot-Rolling Strip Steel [J]. Acta Metallurgica Sinica, 2001, 37(1): 99-103 (in Chinese).

[8] Galuntucci L M, Tricarico L. Thermo-Mechanical Simulation of a Rolling Process With an FEM Approach [J]. Journal of Materials Processing Technology, 1999, 92-93: 494-501.

[9] Komori K. Simulation of Deformation and Temperature in Caliber Rolling: Effect of Finite-Element Mesh in Cross-Section [J]. Journal of Materials Processing Technology, 2003, 143-144: 367-372.

[10] LIU Cai, CUI Zhen-shan. Thermomechanical Coupled Finite Element Modelling of Slab Hot Rolling [J]. Chinese Journal of Mechanical Engineering, 1998, 34(4): 35-39 (in Chinese).

[11] ZHANG Peng, LU Shou-li, GAO Yong-sheng. Numerical Simulation for Hot Shape Rolling Process of Shape Steel With Simple Section [J]. Journal of Iron and Steel Research, International, 1999, 11(3): 25-29 (in Chinese).

[12] ZHOU S X. An Integrated Model for Hot Rolling of Steel Strips [J]. Journal of Materials Processing Technology, 2003, 134(3): 338-351.

[13] LI Chang-sheng, LIU Xiang-hua, WANG Guo-dong, et al. Simulation on Temperature Field in Continuous Bar and Rod Rolling by FEM [J]. Journal of Plasticity Engineering, 1998, 5(2): 79-84 (in Chinese).

[14] LI C X, LIU X H, WANG G D. Simulation on Temperature Field of 50CrV4 Automobile Gear Bar Steel in Continuous Rolling by FEM [J]. Journal of Materials Processing Technology, 2002, 120(1-3): 26-29.